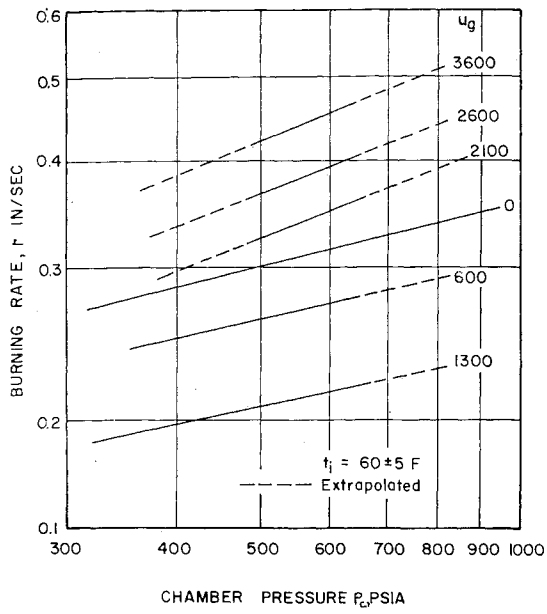

Fig. 4 Burning rate of a solid propellant as a function of chamber pressure with the combustion gas velocity as a parameter.

Figure 2 presents r_0, as a function of p_c for $t_i = -15 \pm 5F$, $60 \pm 5F$, and $100 \pm 5F$. All measurements were made at the same location from the fore-end of the propellant sample.

The values of r_0 determined with the research apparatus differed from those obtained from large rocket motor firings by less than 1%. The burning rates measured with the apparatus, at a given operating condition, were repetitive to within 3%. A minimum of three experiments were conducted at each operating point.[4, 5]

Combustion gas velocity

Table 1 presents the ranges over which u_g and p_c were varied during the investigation. Figure 3 presents the total burning rate r as a function of the combustion gas velocity u_g for the following constant values of combustion pressure: $p_c = 400$, 500, and 600 psia. The values of r measured at a given operating condition were repetitive to within 4%. At each operating point, a minimum of two to four runs were conducted. The curves indicate that for the particular propellant there is a "threshold" velocity u_{tv} above which the observed burning rate r is faster than the linear burning rate r_0; Fig. 3 shows that u_{tv} is a function of p_c.

Figure 4 presents the log$r$ as a function of the logp_c for the following constant values of u_g: 0, 600, 1300, 2100, 2600, and 3600 fps. The curve for $u_g = 0$ corresponds to the linear burning rate r_0 obtained at a propellant temperature $t_i = 60 \pm 5F$.

Propellant temperature

Experiments were conducted for determining the influence of the propellant temperature t_i upon the burning rate r; the latter includes the contribution due to erosive burning. Two different values of propellant temperature were investigated: $t_i = -15 \pm 5$ and $t_i = 100 \pm 5F$. Table 2 presents the results obtained from experiments for determining the influence of t_i.

The data presented in Table 2 indicate that the erosive burning rate r_e is influenced by the initial temperature of the propellant t_i and increases as t_i decreases.

IV. Conclusions

Based on the experiments discussed in this paper, the following conclusions, pertinent to the subject propellant, may be drawn: 1) the photographic technique permits determining the instantaneous (less than 0.1 sec) burning rate r of a solid propellant sample; 2) under erosive burning conditions, the subject solid propellant exhibits a threshold velocity, which is pressure dependent; 3) limited experiments indicate that a decrease in the propellant temperature t_i produces an increase in the erosive burning rate r_e of the propellant.

Table 2 Comparison of burning rates as a function of initial temperature (t_i)

Parameter	$-15F$	$60F$	$60F$	$100F$
Combustion pressure, psia	535	547	652	620
Velocity of the combustion gases, fps	2460	2560	3140	3180
Total burning rate r, in./sec	0.38	0.37	0.42	0.36
Linear burning rate r_0, in./sec	0.28	0.31	0.33	0.32
Erosive burning rate r_e, in./sec	0.10	0.06	0.09	0.04

References

[1] Zucrow, M. J., *Aircraft and Missile Propulsion* (John Wiley and Sons, Inc., New York, 1958), Vol. 2, Chap. 10.

[2] Osborn, J. R., Murphy, J. M., and Kershner, S. D., "Photographic measurement of burning rates in solid propellant rocket motors," Rev. Sci. Instr. **34**, 305–306 (1963).

[3] Murphy, J. M. and Bethel, H. E., "Investigation of new techniques for measuring the burning rate of a solid rocket propellant," Jet Propulsion Center, Purdue Univ. TM-62-8 (October 1962); confidential.

[4] Zucrow, M. J., Osborn, J. R., Murphy, J. M., and Kershner, S. D., "Final report on the investigation of velocity upon burning rate of solid propellants," Jet Propulsion Center, Purdue Univ. Rept. F-63-3 (December 1963); confidential.

[5] Zucrow, M. J., Osborn, J. R., and Murphy, J. M., "The erosive burning of a non-homogeneous solid propellant," 56th Annual AIChE Meeting (December 1963).

Characteristics of Supersonic Ejector Systems with Nonconstant Area Shroud

W. L. Chow* and P. S. Yeh†
University of Illinois, Urbana, Ill.

In our recent studies of supersonic ejector systems,[1, 2] a flow model has been developed stressing the detailed inviscid and viscid interaction between the primary and the secondary streams. The flow phenomena associated with various flow regimes were described and analyzed. The theoretical results thus calculated for ejector systems with cylindrical constant area shrouds were in excellent agreement with those obtained from experiments. This analysis has also been applied to study the starting characteristics of ejector systems.[3] It is intended here to show the applicability of this method to ejector systems with nonconstant area shrouds. The theoretical calculations are only carried out for the "supersonic regime" of the system where the ambient pressure ratio P_a/P_{op} is kept at such low level that it will exert no influence on the flows at the upstream. For the purpose of comparison, experimental results are also obtained for the calculated ejector systems.

Received August 21, 1964. This work was partially supported by NASA as part of a broad research program under Research Grant NsG-13-59. The authors are grateful to H. H. Korst for his continued interest in this problem, and to A. L. Addy for his help in the experimental investigations.

* Associate Professor of Mechanical Engineering. Member AIAA.

† Graduate Research Assistant.

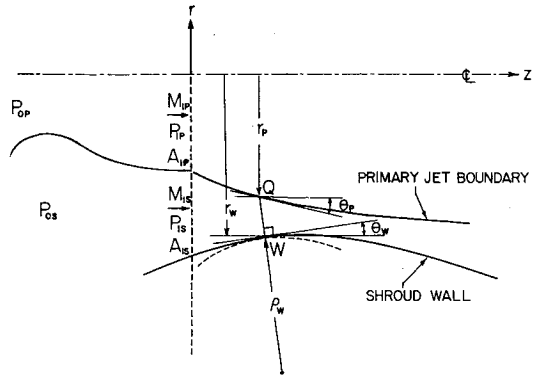

Fig. 1 The axially symmetric supersonic ejector configuration.

To describe briefly the method of calculations, it is recognized that, for the system operating at the supersonic regime, the secondary flow will, in general, reach a sonic condition inside the shroud through the mutual interaction between the streams. The primary flow is calculated by the method of characteristics, and the secondary flow is assumed to follow the one-dimensional isentropic relationship. The mutual interaction between the two streams is based on the fact that the flows have to coexist within the prescribed shroud, and the pressure has to be continuous between them. Thus, for each value of selected initial secondary flow pressure ratio P_{1s}/P_{op}, there corresponds a value of the initial secondary flow Mach number M_{1sl} such that the secondary flow will reach the sonic condition at a location inside the shroud where the secondary flow area is also at a minimum. Within the assumption of one-dimensional flow analysis, the secondary flow area, indicated by line QW in Fig. 1, is given by

$$A_s = \pi(r_w^2 - r_p^2)/\cos\theta_w$$

where the point Q is on the primary jet boundary and the line QW is perpendicular to the tangent of the arbitrary shroud profile at the point W, and the criterion to observe a minimum flow area for the secondary flow is given by

$$\frac{dr_p}{dz} = \left(\frac{r_w}{r_p} + \frac{1}{2r_p}\frac{(r_w^2 - r_p^2)}{\rho_w \cos\theta_w}\right)\frac{dr_w}{dz}$$

where ρ_w is the radius of curvature of the shroud at the point W. The results (M_{1sl} vs P_{1s}/P_{op}) are termed as inviscid solutions.

The viscous effects are then taken into account by superimposing the mixing profiles when the two streams are distinct. Therefore, higher secondary mass rate of flows and larger M_{1sl} values will be resulted. For the regime where the secondary flow rate is extremely small, the mutual interaction and mixing are considered together. (For detailed treatment, see Ref. 1.) This approach will degenerate into Korst's method of base pressure solution[4] when the secondary flow rate is zero.

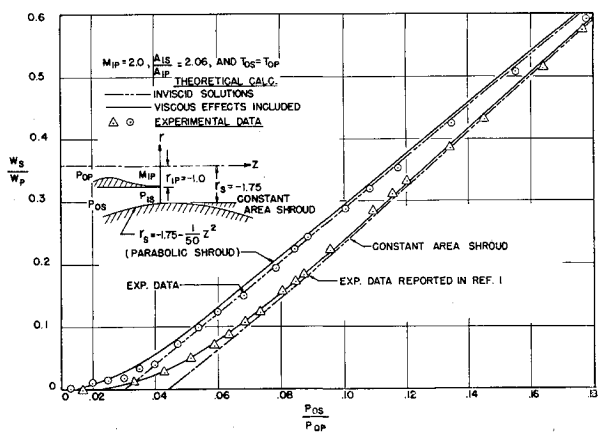

Fig 2 Mass flow rate characteristics of ejector systems in the supersonic regime.

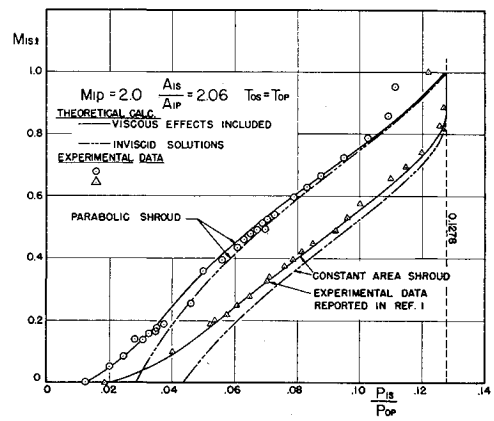

Fig. 3 The limiting initial secondary flow Mach number of ejector systems.

Figures 2 and 3 show the results of calculations‡ obtained for a divergent shroud. For the purpose of comparison, the results for a constant-area shroud that has the same minimum radius are also plotted. It is obvious that the divergence of the shroud would increase the pumping capacity of the ejector system. Figure 4 shows the performance characteristics of the ejector system when the same parabolic shroud is located at various positions relative to the nozzle. The performance curves are essentially displaced with respect to the P_{1s}/P_{op} values, and the "saturated supersonic regime" (i.e., M_{1sl} = 1.0) occurs at much higher values of P_{1s}/P_{op} when the convergent-divergent shroud is displaced toward downstream. Experimental verification of these calculations were also carried out by employing the same system as reported in Ref. 1, and the results are in excellent agreement with the theoretical values.

Of particular interest in the application to "air-augmentation" systems are the pressure distributions along the shroud wall. Figure 5 shows such pressure distributions on the shroud wall when the parabolic shroud is located somewhere downstream as shown. The calculations have been carried

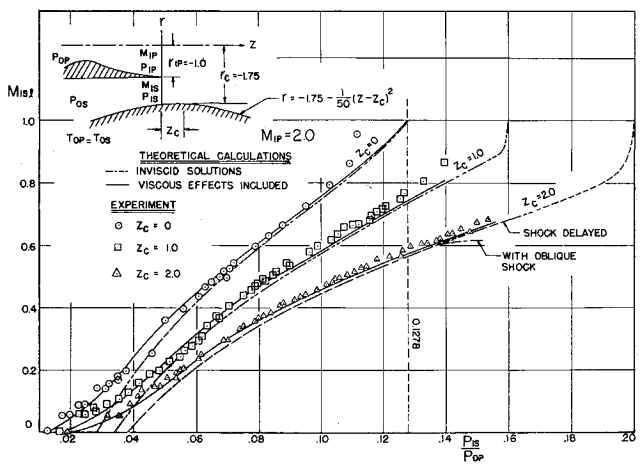

Fig. 4 The effect of location of the shroud on the characteristics of the ejector system.

‡ All calculations reported here were done on IBM-7094 computer system at the University of Illinois.

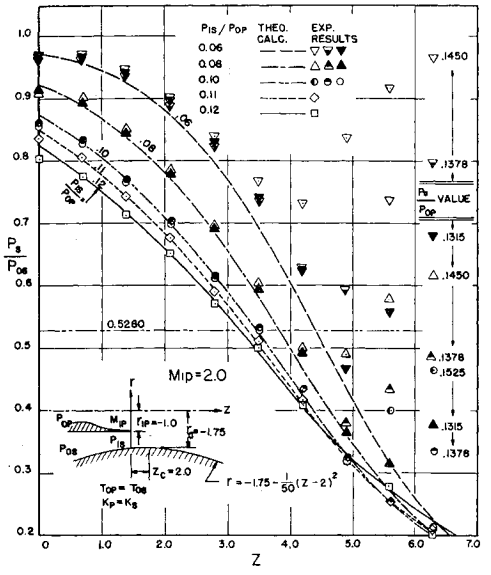

Fig. 5 Pressure distributions on the shroud wall of an ejector system.

out beyond the section where the secondary flow is choked by imposing the secondary stream to be supersonic. The crossover of various constant P_{1s}/P_{op} value curves in this region is reasonable, judging from the fact that an insufficient amount of the secondary flow rate (lower P_{1s}/P_{op} values) at the inlet will result in undesirable overexpansion at the downstream of the ejector-nozzle propulsive systems. Again, the experimental results show very good agreement with the theoretical calculations. Also reported in the same figure is a series of experimental results corresponding to higher ambient pressure ratios P_a/P_{op}§, so that they do not correspond to the supersonic regime. Nevertheless, these results indicate that the system behaves in a manner similar to a convergent-divergent nozzle operating at higher back pressures. It is also interesting to note that, at the various levels of the ambient pressure ratios (corresponding to different high primary stagnation pressures), the results are not much different. One may conclude that, at high Reynolds numbers, the influence of the Reynolds number on the characteristics of the system is indeed negligible.

In the interest of the current development of fluid jet control techniques and devices, this concept of interaction between the primary and secondary streams has also been employed to predict the characteristics of the two-dimensional ejector systems. It is worthwhile to mention that the boundary layer on the side walls of a two-dimensional ejector system may present a predominate modification to the performance of such an ejector system.

References

[1] Chow, W. L. and Addy, A. L., "Interaction between primary and secondary streams of supersonic ejector sytems and their performance characteristics," AIAA J. **2**, 686–694 (1964).

[2] Addy, A. L., "On the steady state and transient operating characteristics of long cylindrical shroud supersonic ejectors (with emphasis on the viscous interaction between the primary and secondary streams)," Ph.D. Thesis, Dept. of Mechanical and Industrial Engineering, Univ. of Illinois (June 1963).

[3] Addy, A. L. and Chow, W. L., "On the starting characteristics of supersonic ejector systems," American Society of Mechanical Engineers Paper 64-FE-9 (1964).

[4] Korst, H. H., "A theory for base pressures in transonic and supersonic flow," J. Appl. Mech. **23**, 593–600 (1956).

§ A detailed study of the effect of this parameter would have to consider the over-all experimental ejector system.

Temperature Effect of Gaseous Hydrogen on Cooling Effectiveness

ALBERT J. HAYEK*
The Marquardt Corporation, Van Nuys, Calif.

Nomenclature

a	=	coolant flow area
c_{pc}	=	coolant specific heat
d_h	=	hydraulic diameter of coolant circuit
h_c	=	coolant-side heat-transfer coefficient
h_g	=	hot gas-side heat-transfer coefficient
k_c	=	thermal conductivity of coolant
k_w	=	thermal conductivity of wall
q/A	=	heat flux
t	=	wall thickness
T_c	=	coolant temperature
T_{wc}	=	coolant-side wall temperature
T_{wh}	=	hot gas-side wall temperature
T_{adwg}	=	hot gas adiabatic wall temperature
w_c	=	coolant flow rate
θ	=	defined by Eq. (6)
μ_c	=	viscosity of coolant
ϕ	=	defined by Eq. (7)

Introduction

MANY ramjet and rocket engine designs use regenerative cooling to maintain the thrust chamber wall at temperatures consistent with good structural integrity. The fuel is generally used as the coolant and is first passed through the coolant circuit, then injected into the combustor as a gas. Hydrogen offers high performance and exceptional cooling qualities; however, any regenerative cooling circuit is limited to the amount of heat it can remove from the engine wall. One method of extending this limit is to design the regenerative cooling circuit so that an optimum coolant temperature occurs at the most critical point in the system. The results of this analysis establish the criteria to determine this optimum coolant temperature.

Analysis

1. *General*

Forced convection cooling is assumed. The coolant-side heat-transfer coefficient is given as[1]

$$h_c = 0.025 \frac{k_c}{d_h} \left(\frac{w_c d_h}{a\mu_c}\right)^{0.8} \left(\frac{c_{pc}\mu_c}{k_c}\right)^{0.4} \left(\frac{T_c}{T_{wc}}\right)^{0.55} \tag{1}$$

Properties of the coolant are based on bulk coolant temperature. The heat flux to the wall is[2]

$$q/A = h_c (T_{wc} - T_c) \tag{2}$$

$$q/A = h_g (T_{adwg} - T_{wh}) \tag{3}$$

$$q/A = (k_w/t)(T_{wh} - T_{wc}) \tag{4}$$

where h_g is calculated using the analysis suggested by Ref. 3. The following assumptions are made: 1) all properties of the hot gas (combustion products) are known, and 2) $T_{wh_{\max}}$ has been established consistent with the wall material chosen. Assumptions 1 and 2 allow the heat flux to the wall to be calculated using Eq. (3). Substituting Eq. (1) into Eq. (2) and solving for w_c yields

$$w_c = [\theta\phi/(T_{wc} - T_c)]^{1.25} (T_c)^{-0.6875} \tag{5}$$

where

$$\theta = \frac{(q/A)\ (d_h)^{0.2}\ (a)^{0.8}\ (T_{wc})^{0.55}}{0.025} \tag{6}$$

Received August 24, 1964.

* Member of the Advanced Technical Staff. Member AIAA.